JOURNAL OF THEORETICAL AND APPLIED MECHANICS
44, 3, pp. 505-532, Warsaw 2006

MODELLING DAMAGE PROCESSES OF CONCRETE AT HIGH TEMPERATURE WITH THERMODYNAMICS OF MULTI-PHASE POROUS MEDIA

Dariusz Gawin

Department of Building Physics and Building Materials, Technical University of Łódź, Poland
e-mail: gawindar@p.lodz.pl

Francesco Pesavento
Bernhard A. Schrefler

Department of Structural and Transportation Engineering, University of Padua, Italy
e-mail: pesa@dic.unipd.it; bas@dic.unipd.it

In this paper, the authors present a mathematical description of a multiphase model of concrete based on the second law of thermodynamics. Exploitation of this law allowed researchers to obtain definitions and constitutive relationships for several important physical quantities, like capillary pressure, disjoining pressure, effective stress, considering also the effect of thin films of water. A mathematical model of hygro-thermo-chemo-mechanical phenomena in heated concrete, treated as a multi-phase porous material, has been formulated. Shrinkage strains were determined using thermodynamic relationships via capillary pressure and area fraction coefficients, while thermo-chemical strains were related to thermo-chemical damage. In the model, a classical thermal creep formulation has been modified and introduced into the model. Results of numerical simulations based on experimental tests carried out at NIST laboratories for two types of concrete confirmed the usefulness of the model in the prediction of the time range, during which the effect of concrete spalling may occur.

Key words: concrete, multiphase, damage, thermal creep

1. Introduction

During heating of concrete, several complex interacting physical and chemical phenomena take place in pores which causes significant changes of its

inner structure and properties (Bazant and Kaplan, 1996; Phan, 1996, Phan *et al.*, 1997; [3]). They can lead to a decrease in the load-bearing capacity or other important service features of concrete structures, especially during a rapid and/or prolonged increase of ambient temperature. A mode of material damage, very specific for concrete at high temperatures, is the so called thermal spalling. This phenomenon has been studied, both experimentally and theoretically, for many years, e.g. Bazant and Kaplan (1996), Bazant and Thonguthai (1978), England and Khoylou (1995), Phan (1996), Phan and Carino (2002), Phan *et al.* (1997, 2001), Sullivan (2001), Ulm *et al.* (1999a,b), [3], but its physical causes are still not fully understood. The reason for such a situation are inherent technical difficulties associated with testing of concrete elements at high temperature, especially when changes of physical properties and several parameters are to be measured simultaneously, the temperature and pressure fields, moisture content, strength properties, intrinsic permeability etc., during experiments at controlled conditions.

Within recent years, the authors of the paper have developed a mathematical model of concrete at high temperatures which considers the porous and multi-phase nature of concrete (Gawin *et al.*, 1999, 2002a,b, 2003, 2004), behaviour of moisture above the critical point of water (Gawin *et al.*, 2002a), load induced thermal strain (Gawin *et al.*, 2004) as well as cracking and thermo-chemical deterioration of concrete (Gawin *et al.*, 2003) and related changes of material properties like, for example, intrinsic permeability (Gawin *et al.*, 2002b). The model has been successfully validated against published results of several experimental tests (Gawin *et al.*, 2003, 2006) showing its sefulness for understanding and predicting of concrete performance at high temperatures.

In this paper, we present the development of model equations taking into account both bulk phases and interfaces, and exploration of the second law of thermodynamics, which allows us to define several quantities used in the model like capillary pressure, disjoining pressure or effective stress, and obtain some thermodynamic restrictions imposed on evolution equations describing material deterioration. Then, we present, as an example of the model application, numerical simulations of experimental tests performed at the NIST laboratories for two types of concrete (Phan, 1996; Phan and Carino, 2002; Phan *et al.*, 1997, 2001), of which only one experienced thermal spalling at prevailing conditions.

2. Mathematical model of concrete at high temperature considered as a multi-phase porous material

The equations of the model are written by considering concrete as a multi-phase porous material, i.e. a medium in which pores are filled by more than one fluid. In the present case, solid skeleton voids are filled partly with liquid water and partly with a gas phase.

Below the critical temperature of water, T_{cr}, the liquid phase consists of physically bound water and capillary water, which appears when the degree of water saturation exceeds the upper limit of the hygroscopic region, S_{ssp}. Above the temperature T_{cr}, the liquid phase consists of bound water only. In the whole temperature range, the gas phase is a mixture of dry air and water vapour, which is a condensable gas constituent for temperatures $T < T_{cr}$.

The constituents are assumed to be chemically non reacting except for the solid phase which is formed by aggregates and products of cement hydration (C-S-H gel and calcium hydroxide, mainly); it is hence affected by the dehydration process for temperatures exceeding about $105°$C. The solid phase is assumed to be in contact with all fluids in the pores.

The global multi-phase system is treated within the framework of averaging theories by Hassanizadeh and Gray (1979a,b, 1980), starting from the microscopic level and applying the mass-, area- and volume averaging operators to the local form of balance equations. As underlined in Schrefler (2002), the interfaces between the constituents and their thermodynamic properties are of importance to consider properly constitutive relationships, thus they are taken into account in the definition of a general form of the model and in the exploitation of the second law of thermodynamics.

For sake of brevity, the microscopic balance equations for the constituents of the porous medium are omitted here as well as the kinematic description. They can be found, e.g. in Lewis and Schrefler (1998).

The set of governing equations at the macroscopic level is as follows (for a detailed description of the procedure see Schrefler (2002)):
— *Mass balance equation for bulk phases and interfaces*

$$\begin{aligned} &\frac{D^{\alpha}\eta^{\alpha}\rho^{\alpha}}{Dt} + \eta^{\alpha}\rho^{\alpha}\,\mathrm{div}\,\boldsymbol{v}^{\alpha} = \sum_{\beta}\widehat{e}^{\alpha}_{\alpha\beta} \\ &\frac{D^{\alpha\beta}a^{\alpha\beta}\Gamma^{\alpha\beta}}{Dt} + a^{\alpha\beta}\Gamma^{\alpha\beta}\,\mathrm{div}\,\boldsymbol{w}^{\alpha\beta} = -\widehat{e}^{\alpha}_{\alpha\beta} - \widehat{e}^{\beta}_{\alpha\beta} + \widehat{e}^{\alpha\beta}_{\alpha\beta\gamma} \end{aligned} \tag{2.1}$$

where $\alpha, \beta = s, w, g$ and $\alpha\beta = sw, sg, wg$ and $\alpha\beta\gamma = swg$.

The mass source terms on the RHS of Eq. $(2.1)_1$ correspond to the exchange of mass with interfaces separating individual phases (phase changes) and couple these equations with the corresponding balance equations written for the interfaces. The last term in Eq. $(2.2)_2$ describes the mass exchange of the interfaces with their contact line. Since we have three phases composing the medium, there is only one contact line. This contact line does not have any thermodynamic properties.

— *Momentum balance equations for the bulk phases and the interfaces*

$$\eta^\alpha \rho^\alpha \frac{D^\alpha \boldsymbol{v}^\alpha}{Dt} - \operatorname{div}(\eta^\alpha \mathbf{t}^\alpha) - \eta^\alpha \rho^\alpha \boldsymbol{g} = \sum_\beta \widehat{\boldsymbol{T}}^\alpha_{\alpha\beta}$$

$$a^{\alpha\beta} \Gamma^{\alpha\beta} \frac{D^{\alpha\beta} \boldsymbol{w}^{\alpha\beta}}{Dt} - \operatorname{div}(a^{\alpha\beta} \mathbf{s}^{\alpha\beta}) - a^{\alpha\beta} \Gamma^{\alpha\beta} \boldsymbol{g}^{\alpha\beta} = \tag{2.2}$$
$$= -(\widehat{\boldsymbol{T}}^\alpha_{\alpha\beta} + \widehat{e}^\alpha_{\alpha\beta} \boldsymbol{v}^{\alpha,s}) - (\widehat{\boldsymbol{T}}^\beta_{\alpha\beta} + \widehat{e}^\beta_{\alpha\beta} \boldsymbol{v}^{\beta,s}) + (\widehat{e}^\alpha_{\alpha\beta} + \widehat{e}^\beta_{\alpha\beta}) \boldsymbol{w}^{\alpha\beta,s} + \hat{\mathbf{s}}^{\alpha\beta}_{\alpha\beta\gamma}$$

The RHS terms in Eq. $(2.2)_1$ describe the supply of momentum from the interfaces, i.e. related to phase changes, while the last RHS term in Eq. $(2.2)_2$ corresponds to the momentum supply from the contact line $\alpha\beta\gamma$ to the $\alpha\beta$ interface. In this equation, $\mathbf{s}^{\alpha\beta}$ is the surface stress tensor, which is symmetric.

— *Energy balance equations for the bulk phases and the interfaces*

$$\eta^\alpha \rho^\alpha \frac{D^\alpha E^\alpha}{Dt} - \eta^\alpha \mathbf{t}^\alpha : \operatorname{grad} \boldsymbol{v}^\alpha - \operatorname{div}(\eta^\alpha \boldsymbol{q}^\alpha) - \eta^\alpha \rho^\alpha h^\alpha = \sum_\beta \widehat{Q}^\alpha_{\alpha\beta}$$

$$a^{\alpha\beta} \Gamma^{\alpha\beta} \frac{D^{\alpha\beta} E^{\alpha\beta}}{Dt} - a^{\alpha\beta} \mathbf{s}^{\alpha\beta} : \operatorname{grad} \boldsymbol{w}^{\alpha\beta} - \operatorname{div}(a^{\alpha\beta} \boldsymbol{q}^{\alpha\beta}) - a^{\alpha\beta} \Gamma^{\alpha\beta} h^{\alpha\beta} = \tag{2.3}$$
$$= -\Big[\widehat{Q}^\alpha_{\alpha\beta} + \widehat{\boldsymbol{T}}^\alpha_{\alpha\beta} \cdot \boldsymbol{v}^{\alpha,\alpha\beta} + \widehat{e}^\alpha_{\alpha\beta}\Big(E^{\alpha,\alpha\beta} + \frac{1}{2}(v^{\alpha,\alpha\beta})^2\Big)\Big] +$$
$$-\Big[\widehat{Q}^\beta_{\alpha\beta} + \widehat{\boldsymbol{T}}^\beta_{\alpha\beta} \cdot \boldsymbol{v}^{\beta,\alpha\beta} + \widehat{e}^\beta_{\alpha\beta}\Big(E^{\beta,\alpha\beta} + \frac{1}{2}(v^{\beta,\alpha\beta})^2\Big)\Big] + \widehat{Q}^{\alpha\beta}_{\alpha\beta\gamma}$$

The source terms in Eq. $(2.3)_1$ describe supply of heat to the bulk phase from the interfaces, related to phase changes. The terms in square brackets in Eq. $(2.3)_2$ describe the energy supply from the bulk phase to the interface, energy associated with the momentum supply and energy related to the mass supply because of phase changes. The last RHS term is the heat supply to the interface from the contact line.

— *Entropy balance equations for the bulk phases and for the interfaces*

The entropy fluxes are defined here as heat fluxes divided by temperature (otherwise a constitutive relationship is needed) and the entropy external

supply due solely to external energy sources is considered, i.e. assuming the hypothesis of simple thermodynamic processes. Thus, the entropy balance for the bulk phases and interfaces may be expressed as follows (Schrefler, 2002))

$$\begin{aligned}
&\eta^{\alpha}\rho^{\alpha}\frac{D^{\alpha}\lambda^{\alpha}}{Dt} - \operatorname{div}\left(\eta^{\alpha}\frac{\boldsymbol{q}^{\alpha}}{T^{\alpha}}\right) - \eta^{\alpha}\rho^{\alpha}\frac{h^{\alpha}}{T^{\alpha}} = \sum_{\beta}\widehat{\Phi}^{\alpha}_{\alpha\beta} + \Lambda^{\alpha} \\
&a^{\alpha\beta}\Gamma^{\alpha\beta}\frac{D^{\alpha\beta}\lambda^{\alpha\beta}}{Dt} - \operatorname{div}\left(a^{\alpha\beta}\frac{\boldsymbol{q}^{\alpha\beta}}{T^{\alpha\beta}}\right) - a^{\alpha\beta}\Gamma^{\alpha\beta}\frac{h^{\alpha\beta}}{T^{\alpha\beta}} = \\
&\quad = -(\widehat{\Phi}^{\alpha}_{\alpha\beta} + \widehat{e}^{\alpha}_{\alpha\beta}\lambda^{\alpha,\alpha\beta}) - (\widehat{\Phi}^{\beta}_{\alpha\beta} + \widehat{e}^{\beta}_{\alpha\beta}\lambda^{\beta,\alpha\beta}) + \widehat{\Phi}^{\alpha\beta}_{\alpha\beta\gamma} + \Lambda^{\alpha\beta}
\end{aligned} \tag{2.4}$$

The first two terms in RHS of Eq. $(2.4)_1$ describe the supply of entropy to the bulk phases from the interfaces, while the last one is the rate of net production of entropy in the bulk phase. The terms in parentheses in the RHS of Eq. $(2.4)_2$ describe the supply of entropy from the interfaces and resulting from the mass supply (phase change), the last but one accounts for the entropy supply to the interface from the contact line and the last one is the rate of net production of entropy in the interface.

The terms related to the exchange of mass, momentum, energy and entropy between interfaces via the contact lines must satisfy some restrictions because the contact lines do not possess any thermodynamic properties as already stated, for further details see Schrefler (2002).

3. The second law of thermodynamics and constitutive relationships

In this section, we explore the second law of thermodynamics, applied for a multi-phase porous medium, whose skeleton experiences chemical reactions (dehydration) and material deterioration (both thermo-chemical and mechanical damage). This allows us to define several important quantities used in our model (e.g. capillary pressure, effective stress tensor) and to obtain some thermodynamic restrictions imposed on the evolution equations for skeleton dehydration and deterioration processes. For sake of brevity, we present here only the main steps of the whole procedure and "abbreviated" form of the equations (but containing all terms used in further developments), which are presented in detail in Schrefler (2002) for finite deformations of the solid skeleton and in Gray and Schrefler (2005) for a more expanded functional

dependence of the internal free energy. All symbols are explained in Nomenclature. For reader's convenience, we have kept the original symbols for the Bishop effective stress and "net" effective stress tensors which were used in Schrefler (2002).

The starting point for further developments is the second law of thermodynamics written for a multi-phase system. It states that for any process, the rate of net entropy production must be non-negative

$$\Lambda = \Lambda^s + \Lambda^w + \Lambda^g + \sum_{\alpha\beta=gs,gw,sw} \Lambda^{\alpha\beta} \geqslant 0 \tag{3.1}$$

After expressing the terms for the rate of net production of entropy in individual phases and interfaces, Eq. (3.1) has the following form (Schrefler, 2002)

$$\begin{aligned}
&(1-n)\rho^s \frac{D^s\lambda^s}{Dt} - \operatorname{div}\Big((1-n)\frac{\boldsymbol{q}^s}{T^s}\Big) - (1-n)\rho^s\frac{h^s}{T^s} - \widehat{\Phi}^s_{sg} + \widehat{\Phi}^s_{sw} \\
&+nS_w\rho^w\frac{D^w\lambda^w}{Dt} - \operatorname{div}\Big(nS_w\frac{\boldsymbol{q}^w}{T^w}\Big) - nS_w\rho^w\frac{h^w}{T^w} - \widehat{\Phi}^w_{wg} - \widehat{\Phi}^w_{ws} + nS_g\rho^g\frac{D^g\lambda^g}{Dt} + \\
&- \operatorname{div}\Big(nS_g\frac{\boldsymbol{q}^g}{T^g}\Big) - nS_g\rho^g\frac{h^g}{T^g} - \widehat{\Phi}^g_{gw} - \widehat{\Phi}^g_{gs} + \sum_{\alpha\beta=gs,gw,sw}\Big[a^{\alpha\beta}\Gamma^{\alpha\beta}\frac{D^{\alpha\beta}\lambda^{\alpha\beta}}{Dt} + \\
&- \operatorname{div}\Big(a^{\alpha\beta}\frac{\boldsymbol{q}^{\alpha\beta}}{T^{\alpha\beta}}\Big) - a^{\alpha\beta}\Gamma^{\alpha\beta}\frac{h^{\alpha\beta}}{T^{\alpha\beta}} + (\widehat{\Phi}^{\alpha}_{\alpha\beta} + \widehat{e}^{\alpha}_{\alpha\beta}\lambda^{\alpha,\alpha\beta}) + \\
&+(\widehat{\Phi}^{\beta}_{\alpha\beta} + \widehat{e}^{\beta}_{\alpha\beta}\lambda^{\beta,\alpha\beta}) - \widehat{\Phi}^{\alpha\beta}_{wgs}\Big] \geqslant 0
\end{aligned} \tag{3.2}$$

In further developments, it is convenient to use the Helmholtz free energy, defined for bulk phases as

$$A^\alpha = E^\alpha - T^\alpha\lambda^\alpha \qquad \alpha = s, w, g \tag{3.3}$$

and for interfaces as

$$A^{\alpha\beta} = E^{\alpha\beta} - T^{\alpha\beta}\lambda^{\alpha\beta} \qquad \alpha\beta = gw, ws, gs \tag{3.4}$$

Introduction of the energy balance equation in the form of Eq. $(2.3)_1$, allows the rate of net production of entropy in the solid phase to be expressed as, see Schrefler (2002)

$$\begin{aligned}
\Lambda^s = &-\frac{(1-n)\rho^s}{T^s}\Big(\frac{D^sA^s}{Dt} + \lambda^s\frac{D^sT^s}{Dt}\Big) + \frac{1-n}{(T^s)^2}\boldsymbol{q}^s\operatorname{grad}T^s + \\
&+\frac{1-n}{T^s}\mathbf{t}^s : \operatorname{grad}\boldsymbol{v}^s - \widehat{\Phi}^s_{sg} - \widehat{\Phi}^s_{sw} + \frac{\widehat{Q}^s_{sw}}{T^s} + \frac{\widehat{Q}^s_{sg}}{T^s}
\end{aligned} \tag{3.5}$$

After similar transformations carried out for all the other phases and for the three interfaces, Eq. $(2.3)_2$, and after application of (3.3) and (3.4), entropy inequality (3.1) can be written as:

$$
\begin{aligned}
&-\frac{(1-n)\rho^s}{T^s}\Big(\frac{D^sA^s}{Dt}+\lambda^s\frac{D^sT^s}{Dt}\Big)-\frac{nS_w\rho^w}{T^w}\Big(\frac{D^wA^w}{Dt}+\lambda^w\frac{D^wT^w}{Dt}\Big)+\\
&-\frac{nS_g\rho^g}{T^g}\Big(\frac{D^gA^g}{Dt}+\lambda^g\frac{D^gT^g}{Dt}\Big)+\\
&+\frac{1-n}{(T^s)^2}\boldsymbol{q}^s\cdot\operatorname{grad}T^s+\frac{nS_w}{(T^w)^2}\boldsymbol{q}^w\cdot\operatorname{grad}T^w+\frac{nS_g}{(T^g)^2}\boldsymbol{q}^g\cdot\operatorname{grad}T^g\\
&+\frac{1-n}{T^s}\mathbf{t}^s:\mathbf{d}^s+\frac{nS_w}{T^w}\mathbf{t}^w:\mathbf{d}^w+\frac{nS_g}{T^g}\mathbf{t}^g:\mathbf{d}^g+\sum_{\alpha\beta=sg,sw,gw}\frac{a^{\alpha\beta}\mathbf{s}^{\alpha\beta}}{T^{\alpha\beta}}:\mathbf{d}^{\alpha\beta}+\\
&-\sum_{\alpha\beta=sg,sw,gw}\frac{a^{\alpha\beta}\Gamma^{\alpha\beta}}{T^{\alpha\beta}}\Big(\frac{D^{\alpha\beta}A^{\alpha\beta}}{Dt}+\lambda^{\alpha\beta}\frac{D^{\alpha\beta}T^{\alpha\beta}}{Dt}\Big)+\sum_{\alpha\beta=sg,sw,gw}\frac{a^{\alpha\beta}}{(T^{\alpha\beta})^2}\boldsymbol{q}^{\alpha\beta}\cdot\nabla T^{\alpha\beta}+\\
&+[\text{terms related to body supplies}]\geqslant 0
\end{aligned}
\tag{3.6}
$$

In this equation, we have introduced strain rate tensors for the bulk phases $\mathbf{d}^\alpha$ $(\alpha=s,w,g)$ and for the interfaces $\mathbf{d}^{\alpha\beta}$ $(\alpha\beta=gw,gs,ws)$. Because of symmetry of the partial stress tensor $\boldsymbol{\sigma}^\alpha$ and the surface stress tensor $\mathbf{s}^{\alpha\beta}$, the following identities hold

$$
\begin{aligned}
&\boldsymbol{\sigma}^\alpha:\operatorname{grad}\boldsymbol{v}^\alpha=\boldsymbol{\sigma}^\alpha:\mathbf{d}^\alpha\\
&\mathbf{s}^{\alpha\beta}:\operatorname{grad}\boldsymbol{w}^{\alpha\beta}=\mathbf{s}^{\alpha\beta}:\mathbf{d}^{\alpha\beta}
\end{aligned}
\tag{3.7}
$$

The Helmholtz free energy for the bulk phases are assumed to have the following functional forms

$$
\begin{aligned}
&A^w=A^w(\rho^w,T^w,S_w) \qquad\qquad A^g=A^g(\rho^g,T^g,S_g)\\
&A^s=A^s(\rho^s,T^s,\boldsymbol{\varepsilon}^s,S_w,\Gamma_{dehydr},D)
\end{aligned}
\tag{3.8}
$$

and for the interfaces

$$
A^{\alpha\beta}=A^{\alpha\beta}(\Gamma^{\alpha\beta},T^{\alpha\beta},a^{\alpha\beta},S_w)\qquad\qquad \alpha\beta=gw,ws,gs \tag{3.9}
$$

One must underline that in Eq. (3.8) for the solid skeleton, the effect of the two internal variables, Γ_{dehydr} and D, has been additionally considered, as compared to Schrefler (2002).

After calculating the material time derivatives of the Helmholz free energies (3.8) and (3.9), the entropy inequality becomes

$$
\begin{aligned}
&-\frac{(1-n)\rho^s}{T^s}\frac{D^sT^s}{Dt}\Big(\frac{\partial A^s}{\partial T^s}+\lambda^s\Big)-\frac{nS_w\rho^w}{T^w}\frac{D^wT^w}{Dt}\Big(\frac{\partial A^w}{\partial T^w}+\lambda^w\Big)+\\
&-\frac{nS_g\rho^g}{T^g}\frac{D^gT^g}{Dt}\Big(\frac{\partial A^g}{\partial T^g}+\lambda^g\Big)+\\
&-\sum_{\alpha\beta=sg,sw,gw}\frac{a^{\alpha\beta}\Gamma^{\alpha\beta}}{T^{\alpha\beta}}\frac{D^{\alpha\beta}T^{\alpha\beta}}{Dt}\Big(\frac{\partial A^{\alpha\beta}}{\partial T^{\alpha\beta}}+\lambda^{\alpha\beta}\Big)+\frac{nS_w}{T^w}(p^w\mathbf{I}+\boldsymbol{\sigma}^w):\mathbf{d}^w+\\
&+\frac{nS_g}{T^g}(p^g\mathbf{I}+\boldsymbol{\sigma}^g):\mathbf{d}^g+\frac{1-n}{T^s}(\alpha p^s\mathbf{I}+\boldsymbol{\sigma}^s):\mathbf{d}^s-\Big[\frac{(1-n)\rho^s}{T^s}\frac{\partial A^s}{\partial\boldsymbol{\varepsilon}^s}\Big]:\mathbf{d}^s+\\
&+\frac{D^sn}{Dt}\Big(\frac{S_wp^w}{T^w}+\frac{S_gp^g}{T^g}-\frac{p^s}{T^s}\Big)+\frac{1-n}{T^s}A_\Gamma\frac{D^s\Gamma_{dehydr}}{Dt}+\frac{1-n}{T^s}Y\frac{D^sD}{Dt}+\\
&+\frac{D^sS_w}{Dt}\Big(\frac{np^w}{T^w}-\frac{np^g}{T^g}-\frac{nS_w\rho^w}{T^w}\frac{\partial A^w}{\partial S_w}+\frac{nS_g\rho^g}{T^g}\frac{\partial A^g}{\partial S_g}-\frac{(1-n)\rho^s}{T^s}\frac{\partial A^s}{\partial S_w}+\\
&-\sum_{\alpha\beta=sg,sw,gw}\frac{a^{\alpha\beta}\Gamma^{\alpha\beta}}{T^{\alpha\beta}}\frac{\partial A^{\alpha\beta}}{\partial S_w}\Big)+\left[\begin{array}{c}\text{terms related to body supplies,}\\ \text{deformation of the interfaces,}\\ \text{phase changes and heat fluxes}\end{array}\right]\geqslant 0
\end{aligned}
\tag{3.10}
$$

The following definitions have been introduced into (3.10):
— macroscopic pressure of the α phase

$$
p^\alpha=(\rho^\alpha)^2\frac{\partial A^\alpha}{\partial\rho^\alpha}\qquad\qquad\alpha=s,w,g \tag{3.11}
$$

— macroscopic interfacial tension of the interface

$$
\gamma^{\alpha\beta}=-(\Gamma^{\alpha\beta})^2\frac{\partial A^{\alpha\beta}}{\partial\Gamma^{\alpha\beta}}\qquad\qquad\alpha\beta=sw,wg,gs \tag{3.12}
$$

— chemical affinity, being the driving force of the chemical reaction, related to the rate of the dehydration extent, $\dot{\Gamma}_{dehydr}=D^s\Gamma_{dehydr}/Dt$, by means of an evolution equation

$$
A_\Gamma=-\frac{\partial A^s}{\partial\Gamma_{dehydr}}\rho^s \tag{3.13}
$$

together with identities

$$
\begin{aligned}
&\operatorname{div}\boldsymbol{v}^\alpha=\mathbf{d}^\alpha:\mathbf{I}\qquad\qquad\alpha=s,w,g\\
&T^{\alpha,s}=T^\alpha-T^s
\end{aligned}
\tag{3.14}
$$

In the LHS of inequality (3.10), there appear quantities in brackets multiplied by: $D^{\alpha}T^{\alpha}/Dt$, $D^{\alpha\beta}T^{\alpha\beta}/Dt$, $\mathbf{d}^{\alpha}$, $\mathbf{d}^{\alpha\beta}$ which are not primary variables. Therefore, the coefficient of these variables must be always zero, because (3.10) is valid for all thermodynamic states. Hence, the following relationships for specific entropies and stress tensors are obtained

$$\begin{aligned} &\lambda^{\alpha} = -\frac{\partial A^{\alpha}}{\partial T^{\alpha}} && \alpha = w, g, s \\ &\lambda^{\alpha\beta} = -\frac{\partial A^{\alpha\beta}}{\partial T^{\alpha\beta}} && \alpha\beta = gw, ws, gs \\ &\mathbf{s}^{\alpha\beta} = \gamma^{\alpha\beta}\mathbf{I} && \boldsymbol{\sigma}^{w} = -p^{w}\mathbf{I} \qquad \boldsymbol{\sigma}^{g} = -p^{g}\mathbf{I} \end{aligned} \tag{3.15}$$

In particular, the total (nominal) stress tensor of the solid phase is defined by Gray and Schrefler (2005):

$$\boldsymbol{\sigma}^{s} = \boldsymbol{\sigma}_{e}^{s} - \overline{\alpha} p^{s}\mathbf{I} \tag{3.16}$$

where

$$\boldsymbol{\sigma}_{e}^{s} = \rho^{s}\frac{\partial A^{s}}{\partial \boldsymbol{\varepsilon}^{s}} \tag{3.17}$$

is the effective stress tensor of the solid phase, $\overline{\alpha}$ is the Biot coefficient,

$$p^{s}(\rho^{s}, T^{s}, E^{s}, S_{w}) = (\rho^{s})^{2}\frac{\partial A^{s}}{\partial \rho^{s}} \tag{3.18}$$

is the "thermodynamic" pressure of the solid phase,

$$Y = -\rho^{s}\frac{\partial A^{s}}{\partial D} \tag{3.19}$$

is the damage energy release rate,

$$\begin{aligned} p^{c} = \frac{T^{wg}}{n}\Big[&-\frac{nS_{w}\rho^{w}}{T^{w}}\frac{\partial A^{w}}{\partial S_{w}} + \frac{nS_{g}\rho^{g}}{T^{g}}\frac{\partial A^{g}}{\partial S_{g}} - \frac{(1-n)\rho^{s}}{T^{s}}\frac{\partial A^{s}}{\partial S_{w}} + \\ &- \sum_{\alpha\beta=sg,sw,gw}\frac{a^{\alpha\beta}\Gamma^{\alpha\beta}}{T^{\alpha\beta}}\frac{\partial A^{\alpha\beta}}{\partial S^{w}}\Big] \end{aligned} \tag{3.20}$$

is the macroscopic 'thermodynamic' capillary pressure, which takes into account the water-gas interface curvature and water film effects.

At the equilibrium state, a stationary condition of the net production of entropy can be imposed, leading to a considerable simplification of the mathematical problem (Schrefler, 2002). Thus, the capillary pressure has the following simplified form

$$p^{c} = p^{g} - p^{w} \tag{3.21}$$

For low moisture contents (i.e. in the hygroscopic region), when water is present only as a thin film on the skeleton surface, it has to be interpreted as the adsorbed water potential Ψ multiplied by the water density ρ^w (Gawin *et al.*, 2002a; Lewis and Schrefler, 1998)

$$p^c = -\Psi\rho^w \qquad \Psi = -\frac{\Delta H_{ads}}{M_w} \tag{3.22}$$

where ΔH_{ads} is the enthalpy of adsorption.

When taking into account the water films explicitly, their pressure p^w differs from the reservoir water pressure, p_o^w, by an amount equal to the disjoining pressure, Π^w, according to the enhanced model of (Gray and Schrefler, 2001)

$$p^w = p_o^w - \Pi^w \tag{3.23}$$

hence, the capillary pressure at the equilibrium is then defined as (Gray and Schrefler, 2001)

$$p^c = p^g - p^w = \Pi^w - \mathbf{s}^{wg} J_{wg}^w \tag{3.24}$$

For higher levels of moisture content, i.e. for saturation values exceeding the solid saturation point, the capillary pressure is

$$p^c = -\mathbf{s}^{wg} J_{wg}^w \tag{3.25}$$

which brings us back to Eq. (3.21).

Similarly, in the hygroscopic region, the thermodynamic solid pressure at the equilibrium can be expressed by a simplified formula neglecting the term related to the thickness of the meniscus surface (valid when the film thickness is smaller than the radius of curvature of the solid particles (Gray and Schrefler, 2001))

$$p^s \cong \chi_s^{ws}(p_o^w - \Pi^w) + \chi_s^{gs} p^g + \chi_s^{ws}\mathbf{s}^{ws} J_{ws}^s + \chi_s^{gs}\mathbf{s}^{gs} J_{gs}^s \tag{3.26}$$

while in the non-hygroscopic region (i.e. for moderate levels of wetting phase saturation)

$$p^s \cong \chi_s^{ws} p^w + \chi_s^{gs} p^g + \chi_s^{ws}\mathbf{s}^{ws} J_{ws}^s + \chi_s^{gs}\mathbf{s}^{gs} J_{gs}^s \tag{3.27}$$

where χ_s^{ws} and χ_s^{gs} are fractions of the skeleton area in contact with water and gas, respectively.

The capillary pressure terms in Eqs. (3.26) and (3.27), accounting for a jump in pressure across the curved surface of the solid, i.e. the last two terms in the RHS of Eqs. (3.26) and (3.27), are typically not included in expressions used for the solid phase pressure in practical applications and are neglected in our model. Taking this into account, together with the definitions of the

capillary pressure at different water saturation levels, Eqs. (3.24) and (3.25), and obvious identity $\chi_s^{ws} + \chi_s^{gs} = 1$, it allows us for writing one common expression for the solid phase pressure in the following form

$$p^s = p^g - \chi_s^{ws} p^c \tag{3.28}$$

It is similar to the commonly used expression developed for partially saturated porous media by Bishop, but it is also valid for materials with very small pores and a well developed internal pore surface, where water can be present as a thin film, like e.g. in concrete Gray and Schrefler (2001).

As far as mechanical constitutive relationships are concerned, we introduce damage into the elastic constitutive law in a classical manner. We consider that only elastic properties of the material are affected by the total damage parameter D, defined by Eq. (3.35) accounting for both mechanical and thermo-chemical damage components, d and V, see Eqs. (3.36), and that the dependence on damage is introduced through the stiffness matrix, $\mathbf{\Lambda} = \mathbf{\Lambda}(D)$

$$\boldsymbol{\sigma}_e^s = \mathbf{\Lambda}(D) : \boldsymbol{\varepsilon}_{el} \tag{3.29}$$

Hence, Y, Eq. (3.19), is a quadratic form, positively defined, since $\partial \mathbf{\Lambda}(D)/\partial D < 0$, i.e. the stiffness decreases for increasing damage.

In fact, considering the second derivative of the Helmholtz free energy and exploiting the Maxwell symmetries, we have

$$\frac{\partial^2 A^s}{\partial D \partial \boldsymbol{\varepsilon}_{el}} = \frac{\partial \mathbf{\Lambda}(D)}{\partial D} : \boldsymbol{\varepsilon}_{el} = \frac{\partial^2 A^s}{\partial \boldsymbol{\varepsilon}_{el} \partial D} = -\frac{\partial Y}{\partial \boldsymbol{\varepsilon}_{el}} \tag{3.30}$$

and integrating the latter expression with respect to $\boldsymbol{\varepsilon}_{el}$, we obtain a quadratic form for the damage energy release rate, Y:

$$Y = -\frac{1}{2} \frac{\partial \mathbf{\Lambda}(D)}{\partial D} : \boldsymbol{\varepsilon}_{el} : \boldsymbol{\varepsilon}_{el} + C \tag{3.31}$$

where C is a constant independent on damage ($C = 0$, since $Y = 0$ for $D = 0$).

Thus, the sufficient condition to satisfy the entropy inequality is

$$\dot{D} = \frac{D^s D}{Dt} \geqslant 0$$

which is satisfied when $\dot{d} \geqslant 0$ and $\dot{V} \geqslant 0$, as can be seen from Eq. (3.35).

In our model, we adopt Mazars' theory of damage (Mazars, 1984, 1989), i.e. the material is supposed to behave elastically and to remain isotropic. Application of the true stress concept (Chaboche, 1988)

$$\boldsymbol{\sigma}_e^s = (1 - D) \tilde{\boldsymbol{\sigma}}_e^s \tag{3.32}$$

where $\widetilde{\boldsymbol{\sigma}}_e^s$ is the "net effective stress" (in the sense of damage mechanics and porous media), leads to the following form of the constitutive relationship for the solid phase

$$\widetilde{\boldsymbol{\sigma}}_e^s = \boldsymbol{\Lambda}_0 : \boldsymbol{\varepsilon}_{el} \tag{3.33}$$

where $\boldsymbol{\Lambda}_0$ is the initial stiffness tensor and $\boldsymbol{\varepsilon}_{el}$ is the elastic strain tensor, see Section 4.

Taking into account $(3.15)_{1,2}$ and (3.30), the "net" effective stress tensor may be expressed as

$$\widetilde{\boldsymbol{\sigma}}_e^s = \frac{\boldsymbol{\sigma}^s + \alpha p^s \mathbf{I}}{1 - D} \tag{3.34}$$

where p^s is given by (3.28). The total damage parameter, D, taking into account a joint action of mechanical and thermo-chemical degradations, can be found from the following relation (Gawin *et al.*, 2003)

$$1 - D = \frac{E(T)}{E_o(T_a)} = \frac{E(T)}{E_o(T)} \frac{E_o(T)}{E_o(T_a)} = (1 - d)(1 - V) \tag{3.35}$$

where the subscript o concerns a mechanically unloaded material. The mechanical and thermo-chemical damage parameters, d and V, are defined on the basis of experimentally determined changes in Young's modulus, E, as follows (Gawin *et al.*, 2003; Nechnech *et al.*, 2001)

$$d = 1 - \frac{E(T)}{E_o(T)} \qquad V = 1 - \frac{E_o(T)}{E_o(T_a)} \tag{3.36}$$

From the second law of thermodynamics, it is possible to obtain also the well known Fick's law, Fourier's law and Darcy's law, which describe diffusion of miscible components (e.g. water vapour and dry air) in the gas phase, heat transfer by conduction and mass transport due to gradient of gas and capillary pressure (Schrefler, 2002).

For the model closure, several thermodynamic relations, e.g. the Kelvin equation, valid because of the assumption about the local equilibrium state, perfect gases law and Dalton's law for the description of the state of gaseous phases and for the description of partial pressure, have been used. For further details, see Gawin *et al.* (2003), Schrefler (2002).

4. Deformations of concrete at high temperature

When a sample of plain concrete or cement stone is exposed for the first time to heating, it exhibits at higher temperatures considerable changes of its dimensions (irreversible in part) (Bazant and Kaplan, 1996; [3]; Gawin *et*

al., 2004; Khoury, 1995). These deformations are caused by several complex physicochemical phenomena, often acting in opposite directions, like thermal expansion, elasto-plastic strains caused by an external stress, shrinkage strains due to drying, development of cracks and their opening, or volume changes due to cement and aggregate dehydration. A part of these deformations is irreversible in nature and remains as residual strains even after cooling of the sample to the ambient temperature. When an external stress is applied to a concrete sample during its heating for the first time, some additional deformations, slowly increasing with time, can be observed. They are usually referred to as thermal creep or load induced thermal strain (LITS), and are very characteristic for concrete (Khoury, 1995). Several mathematical models for strains of concrete at high temperature have been proposed up to now, e.g. Nechnech *et al.* (2001), Pearce *et al.* (2003), Thelandersson (1987), but they are not coherent with the mechanistic approach to the modelling of concrete as a multi-phase porous material, which is adopted in this and our previous works (Gawin *et al.*, 1999, 2002a,b, 2003, 2004), and in particular with application of the effective stresses, defined by Eqs. (3.16) and (3.28), to determine the skeleton strains. We proposed such a model originally in Gawin *et al.* (2004), and for convenience of reader we will briefly summarise it below.

The total strain of mechanically loaded concrete at the temperature T, $\boldsymbol{\varepsilon}_{tot}$, can be split into the following components (Gawin *et al.*, 2004)

$$\boldsymbol{\varepsilon}_{tot}(\widetilde{\boldsymbol{\sigma}}_e^s, T) = \boldsymbol{\varepsilon}_{el}(\widetilde{\boldsymbol{\sigma}}_e^s, T) + \boldsymbol{\varepsilon}_{th}(T) + \boldsymbol{\varepsilon}_{tchem}(V(T)) + \boldsymbol{\varepsilon}_{tr}(\widetilde{\boldsymbol{\sigma}}_e^s, T) \tag{4.1}$$

where $\boldsymbol{\varepsilon}_{el}$ is the elastic strain due to the 'net' effective stresses acting on the load bearing part of the skeleton, $\widetilde{\boldsymbol{\sigma}}_e^s$, and which are caused by the external load and pressure of pore fluids (i.e. liquid water and moist air), $\boldsymbol{\varepsilon}_{th}$ is the thermal strain component, $\boldsymbol{\varepsilon}_{tchem}$ the thermo-chemical strain (irreversible component), and $\boldsymbol{\varepsilon}_{tr}$ the transient thermal strain, called also LITS or thermal creep. We remind that the shrinkage strain is included into the elastic strain component as a result of action of capillary pressure (considering disjoining pressure at lower moisture contents) upon the solid surface fraction being in direct contact with liquid water, $\chi_s^{ws}(S_w)$, dependent on the moisture content, see Eqs. (3.16) and (3.28).

A reversible part of the thermal dilatation of unloaded concrete, called here the thermal strain, $\boldsymbol{\varepsilon}_{th}$, can be obtained from the following incremental relation (Gawin *et al.*, 2004)

$$d\boldsymbol{\varepsilon}_{th} = \beta_s(T)\mathbf{I}\, dT \tag{4.2}$$

with the thermal dilatation coefficient $\beta_s(T)$ depending on the temperature.

Regression analysis performed in Gawin *et al.* (2004) for the experimental data concerning two types of HPC concrete, C-90 and C-60 [3], showed a linear dependence of the coefficient β_s on temperature, with correlation coefficient $R^2 > 0.99$, in the temperature range up to $800°\mathrm{C}$.

In heated concrete, above temperatures of about $105°\mathrm{C}$, there start several complex endothermic chemical reactions, generally called concrete dehydration, e.g. Bazant and Kaplan (1996). They cause thermal decomposition of the cement matrix, and at higher temperatures also of the aggregate (depending on its type and composition), what results in a considerable chemical shrinkage of the cement matrix and usually expansion of the aggregate. Due to these contradictory, or at least incompatible, behaviour of the concrete components, cracks of various dimensions are developing when temperature increases, [3], causing an additional change of concrete strains (usually expansion). It is practically impossible to separate the effects of dehydration and cracking processes during experimental investigations of thermal dilatation of concrete at high temperatures, hence they are considered jointly as thermo-chemical strains, which in an incremental form are given by Gawin *et al.* (2004)

$$d\boldsymbol{\varepsilon}_{tchem} = \beta_{tchem}(V)\mathbf{I}\, dV \tag{4.3}$$

where $\beta_{tchem}(V)$ is the material function to be determined experimentally. It is expressed in terms of the thermo-chemical damage parameter, V, given by Eq. (3.36), which was physically justified in Gawin *et al.* (2004), taking also into account the irreversible nature of these strains.

During first heating, mechanically loaded concrete exhibits greater strains as compared to the load-free material at the same temperature. A part of them originates just from the elastic deformation due to mechanical load, $\boldsymbol{\varepsilon}_{el}(\widetilde{\boldsymbol{\sigma}}_e^s, T)$, and it increases during heating because of thermo-chemical and mechanical degradation of the material. The time dependent part of strains due to transient thermal processes, $\boldsymbol{\varepsilon}_{tr}(\widetilde{\boldsymbol{\sigma}}_e^s, T)$, is generally referred to as thermal creep or Load Induced Thermal Strain (LITS) (Khoury, 1995). Its physical nature is rather complex and up today not fully understood, thus the modelling is usually based on results of special experimental tests, which are performed at constant heating rate for various (but constant during a particular test) levels of material stresses, see e.g. Gawin *et al.* (2004), Khoury (1995), [3].

The transient thermal strains, $\boldsymbol{\varepsilon}_{tr}$, modelled for a multi-axial stress state similarly as in Nechnech *et al.* (2001), Pearce *et al.*, 2003, Thelandersson (1987), can be obtained from the following incremental formula (Gawin *et al.*, 2004)

$$d\boldsymbol{\varepsilon}_{tr} = \frac{\overline{\beta}_{tr}(V)}{f_c(T_a)}\mathbf{Q} : \widetilde{\boldsymbol{\sigma}}_e^s\, dV \tag{4.4}$$

where $f_c(T_a)$ is the concrete compressive strength at the room temperature, and $\mathbf{Q}$ is a fourth order tensor defined as follows

$$Q_{ijkl} = -\gamma\delta_{ij}\delta_{kl} + \frac{1}{2}(1+\gamma)(\delta_{ik}\delta_{jl} + \delta_{il}\delta_{jk}) \tag{4.5}$$

with γ being a material parameter determined from the transient creep test. The material function $\overline{\beta}_{tr}(V)$ must be experimentally determined (Gawin *et al.*, 2004). Due to the rreversible character of transient thermal strains, the function is expressed in terms of the thermo-chemical damage parameter, V, rather than temperature, T, which was previously used in some models, e.g. Nechnech *et al.* (2001), Pearce *et al.*, 2003, Thelandersson (1987).

Application of the proposed model of the thermal strains for the C-90 concrete [3] for different levels of compressive loads (including the load-free case), gave satisfactory predictions of strains, both the total ones and LITS (Gawin *et al.*, 2004).

5. Final form of governing equations

Taking into account the constitutive relationships obtained from the exploitation of entropy inequality and neglecting the presence of interfaces, from the general set of field equations, it is possible to formulate a complete model for the analysis of the thermo-hygro-chemical and mechanical behaviour of concrete exposed to a high temperature.

To describe uniquely the state of concrete at high temperatures, we need 4 primary state variables, i.e. gas pressure, p^g, capillary pressure p^c, temperature, T, and displacement vector, $\boldsymbol{u}$, as well as 3 internal variables describing the advancement of dehydration and deterioration processes, i.e. the degree of dehydration, Γ_{dehydr}, chemical damage parameter, V, and mechanical damage parameter, d. Using the mentioned damage parameters, the total damage parameter, D, can be calculated.

The model consists of 7 equations: 2 mass balances (continuity equations), enthalpy (energy) balance, linear momentum balance (mechanical equilibrium equation) and 3 evolution equations. The final form of model equations, expressed in terms of primary state variables are listed below, after introducing the constitutive relationships. The full development of the equations is presented in Gawin (2000), Gawin *et al.* (2004), Pesavento (2000).

➢ *Mass balance equation of dry air* (involving the solid skeleton mass balance) takes into account both diffusive and advective air flow as well as variations of

porosity caused by the dehydration process and deformations of the skeleton. It has the following form

$$-n\frac{D^sS_w}{Dt} - \beta_s(1-n)S_g\frac{D^sT}{Dt} + S_g \operatorname{div}\boldsymbol{v}^s + \frac{S_g n}{\rho^{ga}}\frac{D^s\rho^{ga}}{Dt} + \frac{1}{\rho^{ga}}\operatorname{div}\boldsymbol{J}_g^{ga} + \\ + \frac{1}{\rho^{ga}}\operatorname{div}(nS_g\rho^{ga}\boldsymbol{v}^{gs}) - \frac{(1-n)S_g}{\rho^s}\frac{\partial\rho^s}{\partial\Gamma_{dehydr}}\frac{D^s\Gamma_{dehydr}}{Dt} = \frac{\dot{m}_{dehydr}}{\rho^s}S_g \tag{5.1}$$

➢ *Mass balance equation of water species* (involving the solid skeleton mass balance) considers diffusive and advective flow of water vapour, mass sources related to phase changes of vapour (evaporation-condensation, physical adsorption – desorption and dehydration), and variations of porosity caused by the dehydration process and deformations of the skeleton, resulting in the following equation

$$n(\rho^w - \rho^{gw})\frac{D^sS_w}{Dt} + (\rho^wS_w + \rho^{gw}S_g)\alpha\operatorname{div}\boldsymbol{v}^s - \beta_{swg}\frac{D^sT}{Dt} + S_g n\frac{D^s\rho^{gw}}{Dt} + \\ + \operatorname{div}\boldsymbol{J}_g^{gw} + \operatorname{div}(nS_w\rho^w\boldsymbol{v}^{ws}) + \operatorname{div}(nS_g\rho^{gw}\boldsymbol{v}^{gs}) + \\ -(\rho^wS_w + \rho^{gw}S_g)\frac{(1-n)}{\rho^s}\frac{\partial\rho^s}{\partial\Gamma_{dehydr}}\frac{D^s\Gamma_{dehydr}}{Dt} = \frac{\dot{m}_{dehydr}}{\rho^s}(\rho^wS_w + \rho^{gw}S_g - \rho^s) \tag{5.2}$$

with β_{swg} defined by

$$\beta_{swg} = \beta_s(1-n)(S_g\rho^{gw} + S_w\rho^w) + n\beta_wS_w\rho^w \tag{5.3}$$

➢ *Enthalpy balance equation of the multi-phase medium* accounting for conductive and convective heat flow and heat effects of phase changes and the dehydration process, can be written as follows

$$(\rho C_p)_{eff}\frac{\partial T}{\partial t} + (\rho_wC_p^w\boldsymbol{v}^w + \rho_gC_p^g\boldsymbol{v}^g)\operatorname{grad}T - \operatorname{div}(\chi_{eff}\operatorname{grad}T) = \\ = -\dot{m}_{vap}\Delta H_{vap} + \dot{m}_{dehydr}\Delta H_{dehydr} \tag{5.4}$$

where χ_{eff} is the effective conductivity found from experiments

$$(\rho C_p)_{eff} = \rho_sC_p^s + \rho_wC_p^w + \rho_gC_p^g \\ \Delta H_{vap} = H^{gw} - H^w \qquad \Delta H_{dehydr} = H^w - H^{ws} \tag{5.5}$$

and

$$\dot{m}_{vap} = -\rho^w S_w \operatorname{div}\frac{\partial \boldsymbol{u}}{\partial t} + \beta_{sw}\rho^w \frac{\partial T}{\partial t} +$$
$$-\rho^w n \frac{\partial S_w}{\partial t} - \operatorname{div}\Big[\rho^w \frac{\boldsymbol{k} k^{rw}}{\mu^w}(-\operatorname{grad} p^g + \operatorname{grad} p^c + \rho^w \boldsymbol{g})\Big] + \tag{5.6}$$
$$-\Big[\dot{m}_{dehydr} + (1-n)\frac{\partial \rho^s}{\partial \Gamma_{dehydr}}\frac{\partial \Gamma_{dehydr}}{\partial t}\Big]\frac{\rho^w S_w}{\rho^s} + \dot{m}_{dehydr}$$

with

$$\beta_{sw} = S_w[(1-n)\beta_s + n\beta_w]$$

and the dehydrated water source is proportional to the dehydration rate

$$\dot{m}_{dehydr} = k_b \dot{\Gamma}_{dehydr} \tag{5.7}$$

k_b is a material parameter related to chemically bound water and dependent on the stoichiometry of chemical reactions associated to the dehydration process.

➢ *Linear momentum conservation equation of the multi-phase medium* has the following form

$$\operatorname{div}(\boldsymbol{\sigma}_e^s - \alpha p^s \mathbf{I}) + \rho \boldsymbol{g} = \mathbf{0} \tag{5.8}$$

where the effective stress $\boldsymbol{\sigma}_e^s$ is given by

$$\boldsymbol{\sigma}_e^s = (1-d)(1-V)\boldsymbol{\Lambda}_0 : (\boldsymbol{\varepsilon}_{tot} - \boldsymbol{\varepsilon}_{th} - \boldsymbol{\varepsilon}_{tchem} - \boldsymbol{\varepsilon}_{tr}) \tag{5.9}$$

with $\boldsymbol{\varepsilon}_{th}$ being the thermal strain given by (4.2), $\boldsymbol{\varepsilon}_{tchem}$ – thermo-chemical strain (4.3), and $\boldsymbol{\varepsilon}_{tr}$ – transient thermal strain (4.4).

➢ *Dehydration process evolution law*, considering its irreversibility, has the form

$$\Gamma_{dehydr}(t) = \Gamma_{dehydr}(T_{max}(t)) \tag{5.10}$$

where $T_{max}(t)$ is the highest temperature reached by concrete up to the time instant t.

The constitutive relationship $\Gamma_{dehydr}(T)$ can be obtained from the results of thermo-gravimetric (TG or DTA) tests, using the definition of the dehydration degree by means of mass changes during concrete heating

$$\Gamma_{dehydr}(T) = \frac{m(T_0) - m(T)}{m(T_0) - m(T_\infty)} \tag{5.11}$$

where $m(T)$ is the mass of concrete specimen measured at the temperature T during TG tests, T_0 and T_∞ are temperatures when the dehydration process starts and finishes. We assumed here $T_0 = 105°\text{C}$ and $T_\infty = 1000°\text{C}$.

➢ *Thermo-chemical damage evolution equation*, obtained from (3.36) on the basis of the experimental results, takes into account the irreversible character of material structural changes and may be written as

$$V(t) = V(T_{max}(t)) \tag{5.12}$$

➢ *Mechanical damage evolution equation*, of the following form

$$d(t) = d(\widetilde{\varepsilon}(t)) \tag{5.13}$$

is expressed in terms of the equivalent strain, $\widetilde{\varepsilon}$, given by equations of the classical non-local isotropic damage theory (Chaboche, 1988; Kachanov, 1958; Mazars, 1984, 1989; Pijaudier-Cabot, 1995). The parameters of the theory can be determined from the results of strength tests ('stress-strain' curves) at various temperatures and the application of first Eq. (3.36), as was done in Gawin *et al.* (2003).

Model equations (5.1)-(5.13) are completed by appropriate constitutive equations and thermodynamic relations, see Gawin (2000), Gawin *et al.* (1999, 2002a, 2003, 2004, 2006).

A numerical solution to the model equations with the finite element method (Lewis and Schrefler, 1998; Zienkiewicz and Taylor, 2000) is presented and discussed in detail in Gawin (2000), Gawin *et al.* (2004, 2006), Pesavento (2000).

6. Numerical simulation of the NIST test at $450°\text{C}$

A comparison between numerical results, obtained by means of the model described in the previous sections, and experimental results from the compressive tests carried out at NIST laboratories (Phan, 1996; Phan and Carino, 2002; Phan *et al.*, 1997, 2001), will be presented here. This demonstrates the capability of the numerical model to assess the risk of thermal spalling in concrete exposed to elevated temperatures.

The main aim of the tests carried out at NIST laboratories was to evaluate the thermo-mechanical behaviour of four different HPCs with different mix

compositions exposed to high temperatures. Cylindrical specimens, all of them with a diameter of 100 mm and height of 200 mm, were tested using different test methods and target temperatures. Herein, our attention is focused on unstressed heating tests to the final target temperature of 450°C for concretes indicated as MIX-1 (with $f_c = 98\,\mathrm{MPa}$, $w/c = 0.22$, $k_0 = 2 \cdot 10^{-19}\mathrm{m}^2$) and MIX-2 ($f_c = 82\,\mathrm{MPa}$, $w/c = 0.33$, $k_0 = 2 \cdot 10^{-18}\mathrm{m}^2$). All MIX-1 specimens and only one of four MIX-2 specimens experienced explosive spalling during the test at these conditions.

During the test, the heating rate was initially equal to 5 K/min and heating was stopped when the temperature in the centre of the specimen was within 10 K of the target temperature T, and the difference between the surface and centre temperatures of the concrete specimen was less than 10 K. For further details concerning the mix compositions and tests procedures (set-up, temperature control, instrumentation of the specimens), see Phan (1996), Phan and Carino (2002), Phan *et al.* (1997, 2001).

Initially, the specimen had temperature $T = 296.15\,\mathrm{K}$ (23°C), gas pressure $p^g = 101325\,\mathrm{Pa}$ and pore relative humidity $\varphi = 50\%\mathrm{RH}$. The results of our simulations are presented in Fig. 1 and Fig. 2.

Figures 1a,b show the evolution of temperature difference, ΔT, between the surface and the centre of specimens measured during the tests and the corresponding numerical values. The accordance between the numerical and experimental results is quite good, except for the initial phase of heating of MIX-1, Fig. 1a, when the experimental profile shows that the temperature difference between the core and surface is practically zero for more than one hour, which was probably caused by some problems with temperature measurement. The same figure shows the history of mechanical damage parameter in the middle of the radius obtained from the simulations. Corresponding to the maximum value of ΔT, a steep increase in the mechanical damage parameter d (with the maximum value $d_{max} =\sim 75\%$) may be observed for MIX-1, Fig. 1a, while much slower increase of d (with $d_{max} =\sim 50\%$) is obtained for MIX-2, see Fig. 1b.

Figures 2a,b show a comparison of behaviour of tested concretes in the space domain. In particular, Fig. 2a shows the comparison of gas pressure distributions in the radial direction at four time stations corresponding to the time range when the thermal spalling was observed during the experimental tests. The maximum values of p^g are concentrated in the critical time range. Then, the pressure tends to diminish rather quickly. Gas pressures in MIX-1 are approximately two times higher than in MIX-2 which has higher permeability due to a higher w/c ratio. At the end of the simulation ($t = 300\,\mathrm{min}$),

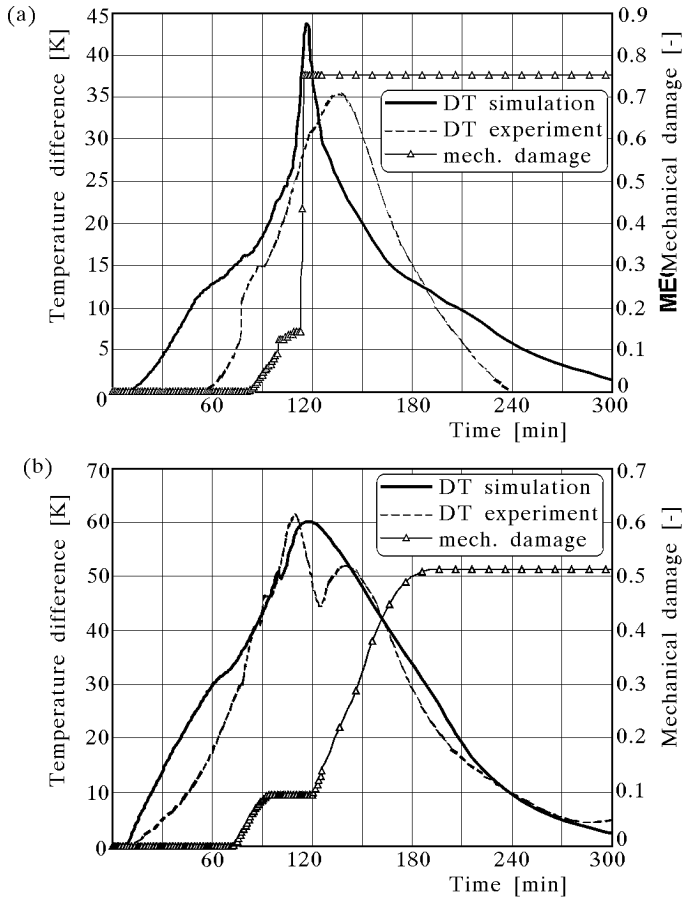

Fig. 1. Time evolution of the mechanical damage parameter and temperature difference in concrete specimens made of two types of the concrete: (a) MIX-1, (b) MIX-2, in a NIST experimental test

it is equal to the atmospheric pressure in the whole specimen. Figure 2b shows the mechanical damage distribution along the radius. The behaviour of MIX-1 during the 'critical stage' is characterized by a significant increase on the damage parameter, which reaches the maximum value very rapidly. For MIX-2, the damage parameter does not exceed 20% which indicates much lower risk of thermal spalling than for MIX-1.

The results of the presented simulations do not indicate directly the thickness of the spalled concrete layer which was approximately equal to 2 cm for MIX-1. However, after application of the spalling indexes proposed in Gawin *et al.* (2006), the position of spalling occurrence can also be predicted with a sufficient accuracy.

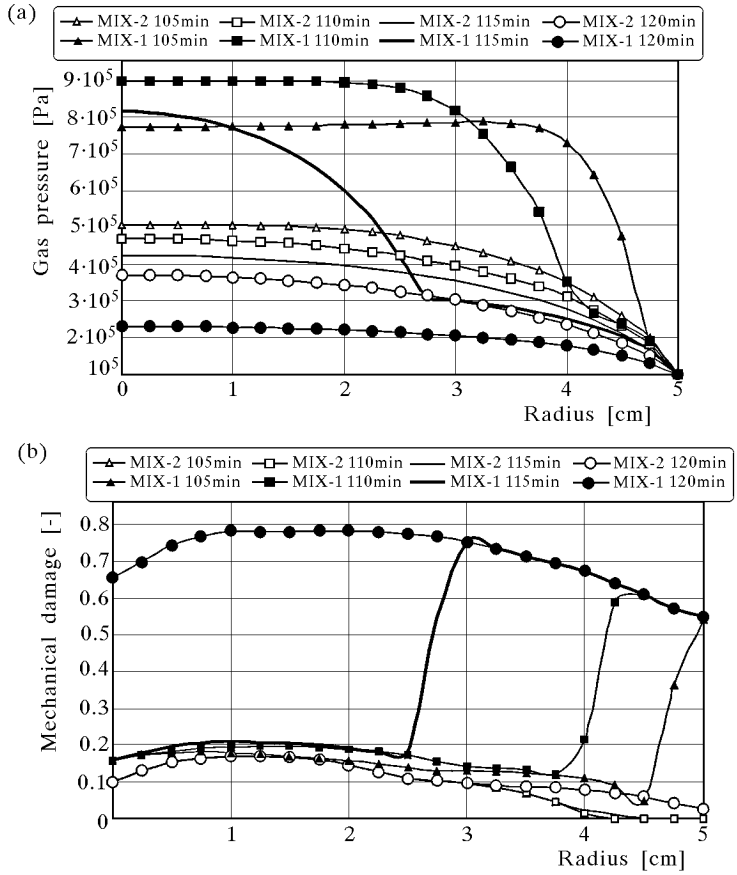

Fig. 2. Comparison of the radial distribution of gas pressure (a) and mechanical damage (b) in concrete specimens made of two types of concrete, MIX-1 and MIX-2, during final stages of the NIST experimental test

After prolonged exposure to a high temperature, the surface layer of concrete elements can be almost completely deteriorated due to stress- and temperature-induced cracking as well as thermo-chemical degradation. Such a case will be characterised in our simulations by high values of the total damage parameter, see e.g. Fig. 8c in Gawin *et al.* (2006). If conditions favouring the previous occurrence of explosive spalling did not appear during heating, one can expect a gradual drop of the external deteriorated layer of concrete, what is sometimes called the progressive spalling. The extent of this phenomenon and its evolution in time can be estimated by means of a kind of "critical value" of the D parameter. A reasonable value for such an analysis seems to be $D \cong 0.9\text{-}0.95$ (Gawin *et al.*, 2006).

7. Conclusions

A mathematical model of hygro-thermo-chemo-mechanical phenomena in heated concrete, treated as a multi-phase porous material, has been formulated taking into account most of the important features of the material behaviour at these conditions. Exploitation of the second law of thermodynamics allowed us to obtain definitions and constitutive relationships for several important physical quantities, like capillary pressure, disjoining pressure, effective stress, considering also the effect of thin films of water. Shrinkage strains have been determined using thermodynamic relationships via capillary pressure and area fraction coefficients, while thermo-chemical strains have been related to thermo-chemical damage. A classical thermal creep formulation, based on experimental results, has been appropriately modified and introduced in the model.

The results of numerical simulations, based on experimental tests for two concretes, confirmed the usefulness of the model in the prediction of the time range when the concrete spalling may occur.

Notation

A^{α} – specific Helmholtz free energy for bulk phase α [$\mathrm{J\,kg^{-1}}$]
$A^{\alpha\beta}$ – specific Helmholtz free energy for interface $\alpha\beta$ [$\mathrm{J\,kg^{-1}}$]
$a^{\alpha\beta}$ – specific surface of $\alpha\beta$-interface [$\mathrm{m^{-1}}$]
C_p – effective specific heat of porous medium [$\mathrm{J\,kg^{-1}K^{-1}}$]
C_p^g – specific heat of gas mixture [$\mathrm{J\,kg^{-1}K^{-1}}$]
C_p^w – specific heat of liquid phase [$\mathrm{J\,kg^{-1}K^{-1}}$]
D – total damage parameter [–]
d – mechanical damage parameter [–]
$\mathbf{d}^{\alpha}$ – strain rate tensor of bulk phase α [$\mathrm{s^{-1}}$]
$\mathbf{D}_d^{gw}$ – effective diffusivity tensor of water vapour in dry air [$\mathrm{m^2s^{-1}}$]
E – Young's modulus [Pa]
$\widehat{e}^{\alpha}_{\alpha\beta}$ – rate of mass transfer to bulk phase α from interface $\alpha\beta$ [$\mathrm{kg\,m^{-3}s^{-1}}$]
$\widehat{e}^{\alpha\beta}_{\alpha\beta\gamma}$ – rate of mass transfer to interface $\alpha\beta$ from contact line $\alpha\beta\gamma$ [$\mathrm{kg\,m^{-3}s^{-1}}$]
E_0 – Young's modulus of mechanically undamaged material [Pa]
E^{α} – internal energy of bulk phase α [$\mathrm{J\,kg^{-1}}$]

$E^{\alpha\beta}$ – internal energy of interface $\alpha\beta$ [$\mathrm{J\,kg^{-1}}$]
$\boldsymbol{g}$ – gravity acceleration [$\mathrm{m\,s^{-2}}$]
H^{α} – enthalpy of bulk phase α [$\mathrm{J\,kg^{-1}}$]
$H^{\alpha\beta}$ – enthalpy of interface $\alpha\beta$ [$\mathrm{J\,kg^{-1}}$]
h^{α} – heat source in bulk phase α [$\mathrm{W\,kg^{-1}}$]
$h^{\alpha\beta}$ – heat source on interface $\alpha\beta$ [$\mathrm{W\,kg^{-1}}$]
$\mathbf{I}$ – unit tensor [–]
$J^{\alpha}_{\alpha\beta}$ – curvature of $\alpha\beta$ interface with respect to bulk phase α [$\mathrm{m^{-1}}$]
$\boldsymbol{J}^{gw}_{d}$ – diffusive flux of vapour [$\mathrm{kg\,m^{-2}s^{-1}}$]
$\boldsymbol{J}^{ga}_{d}$ – diffusive flux of dry air [$\mathrm{kg\,m^{-2}s^{-1}}$]
$\mathbf{k}$ – absolute permeability tensor [$\mathrm{m^2}$]
k – absolute permeability (scalar) [$\mathrm{m^2}$]
$k^{r\pi}$ – relative permeability of π-phase ($\pi = g, w$) [–]
$\dot{m}_{dehydr}$ – rate of mass due to dehydration [$\mathrm{kg\,m^{-3}s^{-1}}$]
$\dot{m}_{vap}$ – rate of mass due to phase change [$\mathrm{kg\,m^{-3}s^{-1}}$]
n – total porosity (pore volume/total volume) [–]
p^{c} – capillary pressure [Pa]
p^{g} – pressure of gas phase [Pa]
p^{w} – pressure of liquid water [Pa]
p^{s} – solid skeleton pressure [Pa]
p^{ga} – dry air partial pressure [Pa]
p^{gw} – water vapour partial pressure [Pa]
$\boldsymbol{q}^{\alpha}$ – heat flux vector for bulk phase α [$\mathrm{W\,m^{-2}}$]
$\boldsymbol{q}^{\alpha\beta}$ – heat flux vector for interface $\alpha\beta$ [$\mathrm{W\,m^{-2}}$]
$\widehat{Q}^{\alpha}_{\alpha\beta}$ – body supply of heat to bulk phase α from interface $\alpha\beta$ [$\mathrm{W\,m^{-3}}$]
$\widehat{Q}^{\alpha\beta}_{\alpha\beta\gamma}$ – body supply of heat to interface $\alpha\beta$ from contact line $\alpha\beta\gamma$ [$\mathrm{W\,m^{-3}}$]
$\mathbf{Q}$ – fourth order tensor for definition of transient thermal strain [–]
S_w – liquid phase volumetric saturation (liquid volume/pore volume) [–]
$\hat{\mathbf{S}}^{\alpha\beta}_{\alpha\beta\gamma}$ – body supply of momentum to $\alpha\beta$-interfaces from $\alpha\beta\gamma$-contact line [$\mathrm{kg\,m^{-2}s^{-2}}$]
$\mathbf{s}^{\alpha\beta}$ – stress tensor for $\alpha\beta$-interface [$\mathrm{Pa\,m}$]
T – absolute temperature [K]
T_{cr} – critical temperature of water [K]
T_{max} – maximum temperature attained during dehydration process [K]
t – time [s]
$\mathbf{t}^{\alpha}$ – partial stress tensor of α-phase [Pa]

$\widehat{\boldsymbol{T}}^{\alpha}_{\alpha\beta}$ – body supply of momentum to bulk phases from interfaces [kg m^{-2}s^{-2}]
$\boldsymbol{u}$ – displacement vector of solid matrix [m]
V – thermo-chemical damage parameter [–]
$\boldsymbol{v}^{\alpha}$ – velocity of α-phase [m s^{-1}]
$\boldsymbol{v}^{gs}$ – relative velocity of gaseous phase [m s^{-1}]
$\boldsymbol{v}^{ws}$ – relative velocity of liquid phase [m s^{-1}]
$\boldsymbol{w}^{\alpha\beta}$ – velocity of interface $\alpha\beta$ [m s^{-1}]

Greek symbols

α – generic bulk phase
$\overline{\alpha}$ – Biot's constant [–]
α_c – convective heat transfer coefficient [W m^{-2}K^{-1}]
$\alpha\beta$ – generic interface of α- and β-phases
β_{tchem} – thermo-chemical strain coefficient [K^{-1}]
β_c – convective mass transfer coefficient [m s^{-1}]
β_s – cubic thermal expansion coefficient of solid [K^{-1}]
β_{swg} – combine (solid + liquid + gas) cubic thermal expansion coefficient [K^{-1}]
β_{sw} – combine (solid + liquid) cubic thermal expansion coefficient [K^{-1}]
$\overline{\beta}_{tr}$ – normalised transient thermal strain coefficient [K^{-1} s]
β_w – thermal expansion coefficient of liquid water [K^{-1}]
χ_s^{ws} – solid surface fraction in contact with the wetting water film [–]
χ_{eff} – effective thermal conductivity [W m^{-1}K^{-1}]
ΔH_{vap} – enthalpy of vaporization per unit mass [J kg^{-1}]
ΔH_{dehydr} – enthalpy of dehydration per unit mass [J kg^{-1}]
$\boldsymbol{\varepsilon}_{el}$ – elastic strain tensor [–]
$\boldsymbol{\varepsilon}_{sh}$ – shrinkage strain tensor [–]
$\boldsymbol{\varepsilon}_{tchem}$ – thermo-chemical strain tensor [–]
$\boldsymbol{\varepsilon}_{th}$ – thermal strain tensor [–]
$\boldsymbol{\varepsilon}_{tot}$ – total strain tensor [–]
$\boldsymbol{\varepsilon}_{tr}$ – transient thermal strain tensor [–]
$\overline{\boldsymbol{\varepsilon}}_{tr}$ – normalized transient thermal strain [–]
$\widetilde{\varepsilon}$ – equivalent strain in damage theory of Mazars [–]
$\Gamma^{\alpha\beta}$ – surface excess mass density of $\alpha\beta$–interface [kg m^{-2}]
Γ_{dehydr} – degree of dehydration [–]
$\gamma^{\alpha\beta}$ – macroscopic interfacial tension of $\alpha\beta$-interface [J m^{-2}]

μ^{π} – dynamic viscosity of constituent π-phase ($\pi = g, w$) [μPa s]
λ^{α} – specific entropy of α-phase [J kg^{-1}K^{-1}]
$\lambda^{\alpha\beta}$ – specific entropy of $\alpha\beta$-interface [J kg^{-1}K^{-1}]
Λ^{α} – rate of net production of entropy of α-phase [W m^{-3}K^{-1}]
$\Lambda^{\alpha\beta}$ – rate of net production of entropy of $\alpha\beta$-interface [W m^{-3}K^{-1}]
$\mathbf{\Lambda}$ – stiffness matrix of damaged material [Pa]
$\mathbf{\Lambda}_0$ – stiffness matrix of undamaged material [Pa]
Π^{w} – disjoining pressure [Pa]
ρ – apparent density of porous medium [kg m^{-3}]
ρ^{g} – gas phase density [kg m^{-3}]
ρ^{w} – liquid phase density [kg m^{-3}]
ρ^{s} – solid phase density [kg m^{-3}]
ρ^{ga} – mass concentration of dry air in gas phase [kg m^{-3}]
ρ^{gw} – mass concentration of water vapour in gas phase [kg m^{-3}]
$\widehat{\Phi}^{\alpha}_{\alpha\beta}$ – body entropy supply to bulk phase α from interface $\alpha\beta$ [W m^{-3}K^{-1}]
$\widehat{\Phi}^{\alpha\beta}_{\alpha\beta\gamma}$ – body entropy supply to interface $\alpha\beta$ from contact line $\alpha\beta\gamma$ [W m^{-3}K^{-1}]
$\boldsymbol{\sigma}$ – Cauchy stress tensor [Pa]
$\boldsymbol{\sigma}^{s}_{e}$ – Bishop effective stress tensor of skeleton [Pa]
$\widetilde{\boldsymbol{\sigma}}^{s}_{e}$ – "net" effective stress tensor of skeleton [Pa]

Acknowledgments

This work was carried out within the framework of the UE project "UPTUN – *Cost-Effective, Sustainable and Innovative Upgrading Methods for Fire Safety in Existing Tunnels*", No. G1RD-CT-2002 00766 and the Italian national project PRIN 2003 No. 2003084345_003 "*Damage and durability mechanics of ordinary and high performance concrete*".

References

1. BAZANT Z.P., KAPLAN M.F., 1996, *Concrete at High Temperatures: Material Properties and Mathematical Models*, Longman, Harlow

2. BAZANT Z.P., THONGUTHAI W., 1978, Pore pressure and drying of concrete at high temperature, *J. Engng. Mech. ASCE*, **104**, 1059-1079

3. Brite Euram III BRPR-CT95-0065 HITECO, Understanding and industrial application of High Performance Concrete in High Temperature Environment – Final Report, 1999

4. CHABOCHE J.L., 1988, Continuum damage mechanics: Part I – General concepts, *J. Applied Mech.*, **55**, 59-64

5. ENGLAND G.L., KHOYLOU N., 1995, Moisture flow in concrete under steady state non-uniform temperature states: experimental observations and theoretical modelling, *Nucl. Eng. Des.*, **156**, 83-107

6. GAWIN D., 2000, *Modelling of Coupled Hygro-Thermal Phenomena in Building Materials and Building Components*, (in Polish), Publ. of Łódź Technical University, **853**

7. GAWIN D., MAJORANA C.E., SCHREFLER B.A., 1999, Numerical analysis of hygro-thermic behaviour and damage of concrete at high temperature, *Mech. Cohes.-Frict. Mater.*, **4**, 37-74

8. GAWIN D., PESAVENTO F., SCHREFLER B.A., 2002a, Modelling of hygro-thermal behaviour and damage of concrete at temperature above the critical point of water, *Int. J. Numer. Anal. Meth. Geomech.*, **26**, 537-562

9. GAWIN D., PESAVENTO F., SCHREFLER B.A., 2002b, Simulation of damage – permeability coupling in hygro-thermo-mechanical analysis of concrete at high temperature, *Commun. Numer. Meth. Eng.*, **18**, 113-119

10. GAWIN D., PESAVENTO F., SCHREFLER B.A., 2003, Modelling of hygro-thermal behaviour of concrete at high temperature with thermo-chemical and mechanical material degradation, *Comput. Methods Appl. Mech. Eng.*, **192**, 1731-1771

11. GAWIN D., PESAVENTO F., SCHREFLER B.A., 2004, Modelling of deformations of high strength concrete at elevated temperatures, *Concrete Science and Engineering – Materials and Structures*, **37**, 268, 218-236

12. GAWIN D., PESAVENTO F., SCHREFLER B.A., 2006, Towards prediction of the thermal spalling risk through a multi-phase porous media model of concrete, *Comput. Methods Appl. Mech. Eng.*, DOI: 10.10.16/j.cma.2005.10.021

13. GRAY W.G., SCHREFLER B.A., 2001, Thermodynamic approach to effective stress in partially saturated porous media, *Eur. J. Mech., A/Solids*, **20**, 521-538

14. GRAY W.G., SCHREFLER B.A., 2005, Analysis of the solid phase stress tensor in multiphase porous media, submitted

15. HASSANIZADEH S.M., GRAY W.G., 1979a, General conservation equations for multi-phase systems: 1. Averaging procedure, *Adv. Water Resources*, **2**, 131-144

16. HASSANIZADEH S.M., GRAY W.G., 1979b, General conservation equations for multi-phase systems: 2. Mass, momenta, energy and entropy equations, *Adv. Water Resources*, **2**, 191-203

17. HASSANIZADEH S.M., GRAY W.G., 1980, General conservation equations for multi-phase systems: 3. Constitutive theory for porous media flow, *Adv. Water Resources*, **3**, 25-40

18. KACHANOV M.D., 1958, Time of rupture process under creep conditions, *Izvestia Akademii Nauk*, **8**, 26-31 (in Russian)

19. KHOURY G.A., 1995, Strain components of nuclear-reactor-type concretes during first heating cycle, *Nuclear Engineering and Design*, **156**, 313-321

20. LEWIS R.W., SCHREFLER B.A., 1998, *The Finite Element Method in the Static and Dynamic Deformation and Consolidation of Porous Media*, Wiley and Sons, Chichester

21. MAZARS J., 1984, *Application de la mecanique de l'endommagement au comportament non lineaire et la rupture du beton de structure*, These de Doctorat d'Etat, L.M.T., Universite de Paris, France

22. MAZARS J., 1989, Description of the behaviour of composite concretes under complex loadings through continuum damage mechanics, *Proc. 10th U.S. National Congress of Applied Mechanics*, J.P. Lamb (edit.), ASME

23. NECHNECH W., REYNOUARD J.M., MEFTAH F., 2001, On modelling of thermo-mechanical concrete for the finite element analysis of structures submitted to elevated temperatures, *Proc. Fracture Mechanics of Concrete Structures*, R. de Borst, J. Mazars, G. Pijaudier-Cabot, J.G.M. van Mier (edit.), 271-278, Swets and Zeitlinger, Lisse

24. PEARCE C.J., DAVIE C.T., NIELSEN C.V., BICANIC N., 2003, A transient creep model for the hygral-thermal-mechanical analysis of concrete, *Proc. Int. Conf. on Computational Plasticity COMPLAS VII* (on CD), Onate E., Owen D.R.J. (edit.), 1-19, CIMNE, Barcelona

25. PESAVENTO F., 2000, *Non-Linear Modelling of Concrete as Multiphase Porous Material in High Temperature Conditions*, Ph.D. Thesis, University of Padova

26. PHAN L.T., 1996, Fire performance of high-strength concrete: a report of the state-of-the-art, *Rep. NISTIR 5934*, p. 105, National Institute of Standards and Technology, Gaitherburg

27. PHAN L.T., CARINO N.J., 2002, Effects of test conditions and mixture proportions on behavior of high-strength concrete exposed to high temperature, *ACI Materials Journal*, **99**, 1, 54-66

28. PHAN L.T., CARINO N.J., DUTHINH D., GARBOCZI E. (EDIT.), 1997, *Proc. Int. Workshop on Fire Performance of High-Strength Concrete*, Gaitherburg (MD), USA, NIST Special Publication 919

29. PHAN L.T., LAWSON J.R., DAVIS F.L., 2001, Effects of elevated temperature exposure on heating characteristics, spalling, and residual properties of high performance concrete, *Materials and Structures*, **34**, 83-91

30. PIJAUDIER-CABOT J., 1995, Non local damage, In: *Continuum Models for Materials with Microstructure*, H.B. Mühlhaus (edit.), Chapt. 4, 105-143, Wiley and Sons, Chichester

31. SCHREFLER B.A., 2002, Mechanics and thermodynamics of saturated-unsaturated porous materials and quantitative solutions, *Applied Mechanics Review*, **55**, 4, 351-388

32. SULLIVAN P.J.E., 2001, Deterioration and spalling of high strength concrete under fire, Offshore Technology Report 2001/074, p. 77, HSE Books, Sudbury

33. THELANDERSSON S., 1987, Modeling of combined thermal and mechanical action on concrete, *J. Eng. Mech. ASCE*, **113**, 6, 893-906

34. ULM F.-J., ACKER P., LEVY M., 1999a, The "Chunnel" fire. II. Analysis of concrete damage, *J. Eng. Mech. ASCE*, **125**, 3, 283-289

35. ULM F.-J., COUSSY O., BAZANT Z., 1999b, The "Chunnel" fire. I. Chemoplastic softening in rapidly heated concrete, *J. Eng. Mech. ASCE*, **125**, 3, 272-282

36. ZIENKIEWICZ O.C., TAYLOR R.L., 2000, *The Finite Element Method, Vol. 1: The Basis*, Butterworth-Heinemann, Oxford

Modelowanie procesów zniszczenia betonu w wysokich temperaturach za pomocą termodynamiki ośrodków porowatych

Streszczenie

Autorzy pracy prezentują równania modelu wielofazowego betonu wyprowadzone na podstawie II zasady termodynamiki. Zastosowanie tej zasady pozwoliło badaczom na sformułowanie definicji i związków konstytutywnych dla kilku ważnych wielkości fizycznych, takich jak: ciśnienie kapilarne, ciśnienie rozklinowywujące, naprężenie efektywne oraz na uwzględnienie efektu wywoływanego przez cienkie warstwy wody obecnej w betonie. Przedstawiono model matematyczny higro-termo-chemomechanicznych zjawisk zachodzących w podgrzewanym betonie traktowanym jako ośrodek porowaty. Skurcz betonu określono za pomocą równań termodynamiki opisujących ciśnienie kapilarne i współczynniki udziału powierzchniowego, podczas gdy odkształcenia termochemiczne skorelowano z parametrem zniszczenia chemicznego. Do rozważań wprowadzono zmodyfikowaną teorię pełzania opartą na sformułowaniu klasycznym. Wyniki przeprowadzonych symulacji numerycznych, bazujących na badaniach doświadczalnych zrealizowanych w laboratoriach NIST na dwóch typach betonu, potwierdziły użyteczność zaprezentowanego modelu w przewidywaniu przedziału czasu, w którym może dojść do termicznego odpryskiwania betonu.

Manuscript received December 28, 2005; accepted for print April 4, 2006